

# Investigation of fuel properties and engine analysis of *Jatropha* biodiesel of Kenyan origin

**Paul Maina**

*Mechanical and Production Engineering Department, Moi University, Kenya*

## **Abstract**

*Biodiesel was produced from *Jatropha curcas* oil of Kenyan origin through a two-step acid-base catalytic transesterification process. The relevant physico-chemical properties of the produced biodiesel were tested according to appropriate standards and were found to be within the requirements. Engine tests were carried out in an Audi, 1.9 litre, turbocharged direct injection, compression ignition engine at different loads. Emissions were measured by a Horiba emission analyser system while combustion data was collected by a data acquisition system, from which, cylinder pressure and rate of heat release of the test engine in every crank angle were calculated. Though the biodiesel had slightly higher brake specific fuel consumption when compared to fossil diesel, its emission behaviour was significantly better. The combustion characteristics were also slightly higher as compared to fossil diesel. This study therefore concluded that biodiesel derived from *Jatropha curcas* of Kenyan origin can be utilized as a safe substitute for mineral diesel.*

*Keywords: biodiesel, engine tests, fuel properties, *Jatropha**

## **1. Introduction**

### **1.1 General introduction**

As petroleum prices continue to rise and concern for the environment grows, alternatives for diesel fuel becomes paramount. Scientists have invested considerable effort in searching for renewable substitutes of diesel fuel. Biodiesel, a mixture of mono alkyl esters of long chain fatty acids, is derived from renewable lipid feedstock, such as vegetable oil or animal fat. Biodiesel can be used in diesel engines without major modifications. It is becoming one of the fastest growing fuels in the global fuel market. It

offers many advantages such as; it is renewable, energy efficient, nontoxic, sulphur free, biodegradable, allows cleaner combustion and reduces global warming gas emissions. Specifically, the combustion of biodiesel from vegetable oil does not add the net CO<sub>2</sub> to the atmosphere because the next crop will re-use the CO<sub>2</sub> to grow.

Biodiesel can be produced from both edible and non-edible plants, however, the major hindrances in widespread application of biodiesel from edible oils and fats are strains in food production, price and availability. On the other hand, non-edible biodiesel feedstocks are easily available in developing countries and are very economical compared to edible oils (Demirbas, 2008). Vegetable oils are important especially in the rural areas of developing countries like Kenya, where there is vast unutilized land in which edible crops cannot thrive and lack modern forms of energy.

### **1.2 Current status of biodiesel in Kenya**

Very little research has been conducted on biodiesel production and tests from agricultural African countries like Kenya, which currently do not have any known commercial reserves for fossil fuels despite the government effort in exploring possible areas. Therefore, all liquid fuels are imported into the country, which is expensive and consume a big percentage of the country's foreign exchange.

Production and use of biodiesel in Kenya is still in its early stages and minimal research has been done in this sector despite the country's potential to produce this fuel. This is against the aims of Kenya to use biodiesel as a substitute for conventional diesel and other fossil fuel sources as well as for export by the year 2020 (Mogaka et al., 2010). Very few researchers have done an in-depth analysis of biodiesel produced from Kenyan feedstocks. These feedstocks include croton megalocarpus (Aliyu et al., 2011, Aliyu et al., 2010) and yellow oleander (Keriko, 2007). Other researchers only characterized the oils e.g. moringa oleifera (Tsaknis. et al.,

1999), *Calodendrum capense*, *Croton megalocarpus*, *Jatropha curcas* and *Cocos nucifera* (Wagutu et al., 2009), while others just mentioned castor oil, *croton megalocarpus*, *Jatropha curcas* and grain *amaranthus* as other oils in Kenya but without any practical analysis (Keriko, 2007).

### 1.3 Aim of study

It is a known fact that the type of biodiesel produced from vegetable oil depends on the type of vegetable oil and its geographical location. For instance, several researchers found that *Jatropha* oil produces superior biodiesel compared to many other non-edible feedstocks (Makkar and Becker, 2009, Treese et al., 2010, Pramanik, 2003) and biodiesel of different origins differs in properties and characteristics as indicated in the research of Emil et al., (2010), Lu et al., (2009) and Foidl et al., (1996) (*Jatropha* seed oil), and Lelas and Tsaknis (2002) (*Moringa oleifera* oil).

The current research deals with the production, analysis and characterization of biodiesel from Kenyan *Jatropha curcas* oil. Short term combustion characteristics, engine performance and emission analysis of this biodiesel was also performed to evaluate its behaviour in an engine. *Jatropha curcas*, which produces a non-edible vegetable oil, is a large shrub or small tree of the family *Euphorbiaceae*. In Kenya, it is naturalized in bush lands and along rivers in western, central and coastal parts of the country at altitudes of 0-1650 meters above sea level (Tomomatsu and Swallow, 2007). So far, no study has reported an in-depth analysis (in terms of fuel characterization and full engine tests) of biodiesel produced from *Jatropha* oils of Kenyan origin.

## 2. Materials and equipment

### 2.1 Material used

*Jatropha curcas* oil was supplied from the Kitui region, Kenya. The chemicals used were analytical reagents; potassium hydroxide and methanol, at 85% and 99.5% purity respectively, and were sourced from local suppliers. The Free Fatty Acids (FFA) were determined by using the simple titration method as per literature (Knothe et al., 2005).

### 2.2 Biodiesel production and property measurements

The transesterification process was preferred for biodiesel production in this study, where the experiments were conducted using beakers as reactors. The reaction beaker was placed on a thermostatically controlled heating plate equipped with a magnetic stirrer. The heating plate had a maximum heating capacity of 420 °C and a maximum agitation of 2000 rpm. A thermometer, held by a retort stand was immersed in the beaker to verify the temperature of the reaction mixture. Fuel properties of

the samples were tested according to the standards recorded in Table 1.

The free fatty acid content of *Jatropha* oil in this study was initially found to be 5.6%. An acid esterification process followed by the transesterification method was then used to prepare the *Jatropha curcas* methyl esters (JCME). The acid pre-treatment process was intended to convert the free fatty acid to esters using an acid catalyst ( $H_2SO_4$ ) to reduce the free fatty acid concentration of the oil to below 1%. The acid catalyst (w/w of oil: 0.5%  $H_2SO_4$ ) and 6:1 methanol/oil molar ratio was used and the mixture stirred at 500 rpm for 1 hour at 50 °C, then after settling, the pre-treated oil was collected and purified (Ramadhas et al., 2005a).

After acid esterification, the transesterification was carried out at the following standard conditions: 6:1 methanol/oil molar ratio (mol/mol), 1.0 wt% potassium hydroxide, 55-60 °C reaction temperature, 400 rpm agitation speed and 60 minutes reaction time (Rashid et al., 2008). After the reaction and settling, the biodiesel (methyl esters) was collected and purified from all impurities. The final product, that is, the biodiesel, formed as a clear, light yellow liquid.

**Table 1: Methods for determination of fuel properties**

Property	Units	Test method
Cetane number	-	ASTM D613
Heating value	MJ/kg	ASTM D240
Density	kg/m <sup>3</sup>	ASTM D941
Viscosity	mm <sup>2</sup> /s	ASTM D445
Flash point	°C	ASTM D93-94
Water content	%	ISO 12937
Acid value	mg KOH/g	ASTM D974
Cloud point	°C	ASTM D2500
Lubricity	µm	ISO 12156
Oxidation stability	h	EN 14112

The fatty acid composition of biodiesel was analysed using a gas chromatography mass spectroscopy (Agilent 6890N) coupled to an inert mass-selective detector (Agilent 5973). The percentage composition of the individual components was obtained from electronic integration measurements using flame ionization detection. All relative percentages determined by GC for each fatty acid sample are the mean of three runs.

### 2.3 Engine tests equipment

An Audi, 1.9 L, turbocharged direct injection (TDI) compression ignition (CI) engine (Figure 3) was used in this experiment. It is a four-stroke, four-cylinder, water cooled diesel engine. Table 2 records the engine's technical specifications.

**Table 2: Experimental engine details**

Engine model	Audi, 1.9 L, TDI
Capacity	1896 cm <sup>3</sup>
Bore	79.5 mm
Stroke	95.5 mm
Compression ratio	19.5:1
Maximum power	66 kW, at 4000 rpm
Maximum torque	202 Nm, at 1900 rpm
Fuel system	Direct injection with electronic distributor pump

Figure 1 depicts the equipment connections for the engine test. The engine (1) was coupled with a dynamometer (2) to provide brake load, while the engine throttling and dynamometer settings were controlled by a computer (9). A pressure transducer (10) was installed in one of the piston cylinders. Cylinder pressure signals from pressure transducer were amplified by a charge amplifier (12), and connected to the SMETech COMBI-PC indication system (8) for data acquisition. The data acquisition system was externally triggered 1024 times in one revolution by an incremental crank angle transducer-optical encoder (11). Fuel was introduced from a fuel tank (3) equipped with flow measurement system. During fuel switching, the fuel tank was drained from the engine fuel filter, new fuel was introduced into the tank until the fuel filter was full, and the engine was then started and allowed to run for a few minutes to clear fuel lines and stabilize.

Emission was measured by Horiba emission analyser system (5) equipped with analyser modules NDIR (AIA-23), H.FID (FIA-22), and H.CLDC (CLA-53M) for measuring (CO, CO<sub>2</sub>, and HC), (THC), and (NO<sub>x</sub>) respectively and a smoke meter (6) connected before the oxidative converter at the

engine exhaust pipe (4). The system was connected to the computer (7), and emission data recorded.

### 2.3 Heat release calculations

During the engine test, the engine was run at constant speed, 3000 rpm, at different loads, from a low idle to 100% load at intervals of 25% of full load. Heat release was subsequently calculated from cylinder pressure and crank angle readings, and emission data was then collected. The net heat release is calculated by a computer program using equation 1 from pressure data (collected with respect to the crank angle) and cylinder geometry with respect to the crank angle. The analysis was derived from the first law of thermodynamics for an open system which is quasi static (Ren *et al.*, 2008):

$$\frac{dQ_n}{d\theta} = \frac{1}{\gamma - 1} \left( \gamma p \frac{dV}{d\theta} + V \frac{dp}{d\theta} \right) \quad (1)$$

Where:

$\frac{dQ_n}{d\theta}$  = Net heat-release rate (J/Degree crank angle).

$\gamma$  = The ratio of specific heats,  $\frac{c_p}{c_v}$

$V$  and  $\frac{dV}{d\theta}$  terms are calculated as shown in equation 2 and equation 3 respectively.

$$V = V_c + A \times r \left[ 1 - \cos\left(\frac{\pi\theta}{180}\right) + \frac{1}{\lambda} \left\{ 1 - \sqrt{1 - \lambda^2 \sin^2\left(\frac{\pi\theta}{180}\right)} \right\} \right] \quad (2)$$

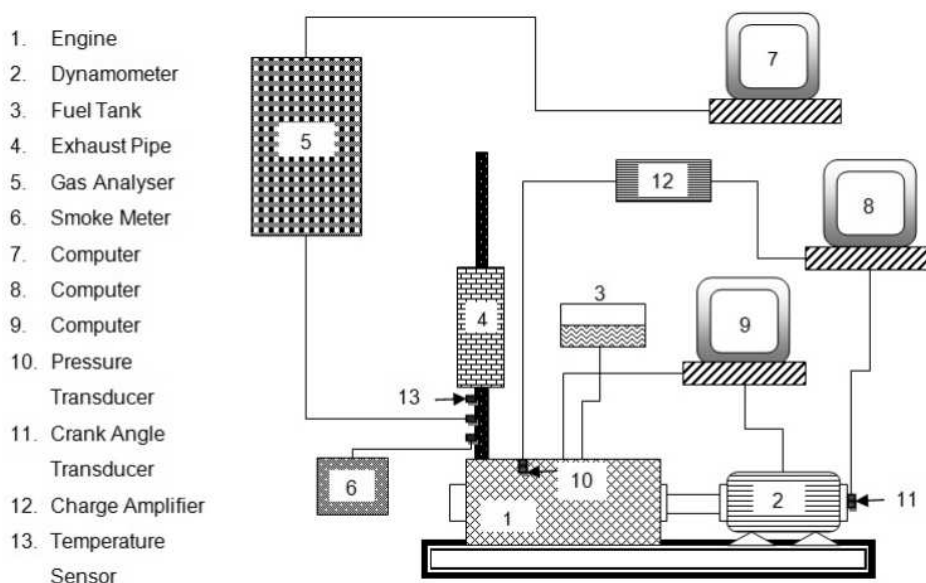


**Figure 1: Engine test experimental set up**

And

$$\frac{dV}{d\theta} = \frac{\pi\theta}{180} \times r \left[ \sin \frac{\pi\theta}{180} + \frac{\lambda^2 \sin^2 \left( \frac{\pi\theta}{180} \right)}{2 \times \sqrt{1 - \lambda^2 \sin^2 \left( \frac{\pi\theta}{180} \right)}} \right] \quad (3)$$

$$\text{But: } \lambda = \frac{l}{r} \text{ and } A = \frac{\pi}{4} D^2$$

Where:

$l$  = Connecting rod length.

$r$  = Crank radius.

$D$  = Cylinder bore.

$V_c$  = Clearance volume.

### 3. Results and discussion

#### 3.1 Biodiesel composition

The fatty acid profiles are the major indicators of the properties of any biodiesel. In this work, biodiesel from jatropha curcas (JCME) had a fatty acid composition as depicted in Table 3. The composition of the fatty acids affects various properties of biodiesel, such as oxidation stability, low temperature flow properties and lubricity.

**Table 3: Fatty acid composition of JCME**

Fatty acid composition (wt. %)	JCME
Palmitic methyl ester (C16/0)	15.3
Palmitoleic methyl ester (C16/1)	1.1
Stearic methyl ester (C18:0)	6.4
Oleic methyl ester (C18/1)	40.1
Linoleic methyl ester (C18/2)	36.9
Linolenic methyl ester (C18/3)	0.2
Saturated fatty acids methyl esters (SFA)	21.7
Monounsaturated fatty acids methyl esters	41.2
Polyunsaturated fatty acids methyl esters	37.1

**Table 4: Fuel properties of biodiesel, diesel and biodiesel standards**

Property	Units	JCME	Diesel	ASTM D6751	EN 14214
Density @ 15 °C	Kg/m <sup>3</sup>	855	832	-	860-900
Viscosity @ 40 °C	mm <sup>2</sup> /s	4.43	3.01	1.9-6.0	3.5-5.0
Acid value	mgKOH/g	0.09	-	0.8 maximum	0.5 maximum
Flash point	°C	186	-	130 minimum	101 minimum
Heating value	MJ/kg	37.82	42.63	-	-
Lubricity	μm	218	-	-	-
Cetane number	-	56.54	54.60	47 minimum	-
Cloud point	°C	1	-16	-	-
Pour point	°C	-3	-19	-	-
Water content	ppm	460	50	500 maximum	500 maximum
Sulphur content	ppm	0.0025	45	-	-
Oxidation stability at 110 °C h	-	9.65	-	-	6 minimum

#### 3.2 Biodiesel properties

Table 4 summarizes the properties of methyl esters from the oil. The properties of fossil diesel are included for comparison purposes. These properties indicate the suitability of methyl esters in this study as an alternative fuel for diesel engines. Properties of the methyl ester from the oil were found to be within the limits of biodiesel standards (ASTM D6751 and EN 14214).

#### 3.3 Brake specific fuel consumption

Figure 2 illustrates the brake specific fuel consumption (BSFC) of the fuel samples tested with respect to different loads. It is defined as the fuel consumption rate divided by its corresponding engine power output. It can be observed that BSFC decreases as the load increases for all fuel samples. This could be caused by the increased air pressure at higher loads; the air pressure in the intake manifold increases as the load increases owing to the increased power of the turbocharger (high exhaust gas volume, flow and temperature) hence the reduced amount of fuel per unit power produced. From the results, it was observed that pure diesel fuel (D2) had the lowest BSFC, approximately 10% lower than that of jatropha curcas methyl ester (JCME) at full load. The higher BSFC of JCME and jatropha curcas oil (JCO) means that more fuel was consumed and less power was produced. This was expected because of the lower heating value (HV) of JCME and JCO compared to D2, at the same time, their higher density also contributed to higher BSFC. At zero load, JCME and JCO had lower BSFC probably because intrinsic oxygen contained in the fuels improved combustion at no load.

#### 3.4 Exhaust gas temperature

Figure 3 depicts the variation of exhaust gas temperature (EGT) versus loads for test fuels. The EGT increases with increasing load. The EGT of JCO was lower than that of JCME (except at zero load). The EGT of JCME was in turn lower compared to

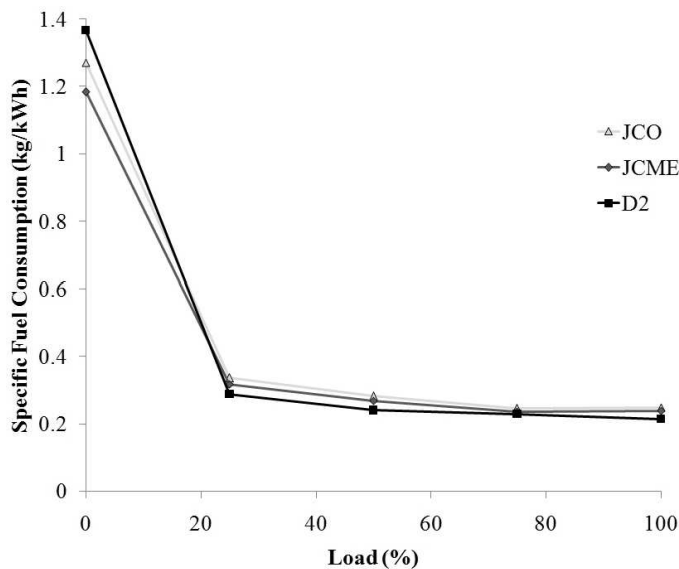


**Figure 2: BSFC for different fuel samples at different loads**

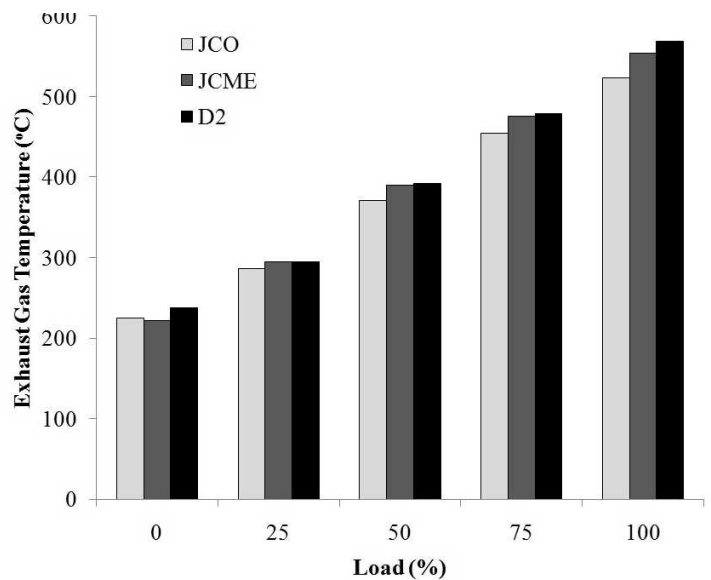


**Figure 3: EGT for different fuel samples at different loads**

that of D2. This might be attributed to the heating value of the fuels. The higher the heating value, the higher the exhaust temperature and vice versa.

### 3.5 Elements present in fuels (C, H, and O)

Figure 4 depicts the major elements carbon, hydrogen and oxygen (C, H and O) contained in fuel samples. It can be observed from the figure that C is the most dominant element in the fuel samples, with the minimum amount being observed in JCME. The amount of H contained is fairly similar for all samples, with JCME recording the highest content. D2 fuel contains the highest C, while JCME and JCO have similar O content. Oxygen is an important element in combustion in that its content influences the stoichiometric air-fuel ratio during the combustion process. A correct amount of in-bound oxygen in a fuel contributes to its better combustion. A high cetane number and presence of intrinsic oxygen in the fuel could result in emission reduction because more complete combustion will consume more of the ignitable mixture formed in the combustion chamber; hence carbon monoxide and hydrocarbon emissions will be reduced.

### 3.6 Emissions

Engine emissions which were experimentally obtained are plotted against load as further described.

#### 3.6.1 Oxides of nitrogen ( $NO_x$ )

Figure 5 depicts the oxides of nitrogen ( $NO_x$ ) emissions of different fuel samples tested at different load conditions. In general, the formation of  $NO_x$  is affected by the peak flame temperature, the high burning gas temperature, the ignition delay and the content of nitrogen and oxygen available in the reaction mixture (Heywood, 1998). It was observed

that as the load increases, the in-cylinder temperature also increases and thus higher absolute  $NO_x$  (ppm) formation results.

Higher cylinder pressure could contribute to increased  $NO_x$  emissions, due to the increased peak combustion temperature at higher engine loads. The results conform to those in the literature (Purushothaman and Nagarajan, 2009b; Purushothaman and Nagarajan, 2009a). D2 exhibited slightly higher  $NO_x$  emissions compared to JCME, especially at lower engine loads, however, JCO had the highest overall emission of  $NO_x$ . The possible reason for this may be the slow burning of the more viscous biodiesel, due to the residence time of the fuel in the high temperature zone being higher. Moreover, the  $NO_x$  emission increase can be associated with the oxygen content in the fuel samples

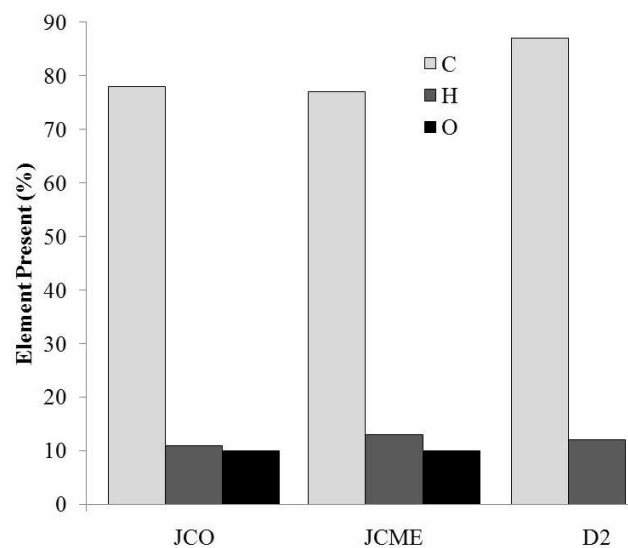


**Figure 4: Contents of elements (C, H, and O) in fuel samples**

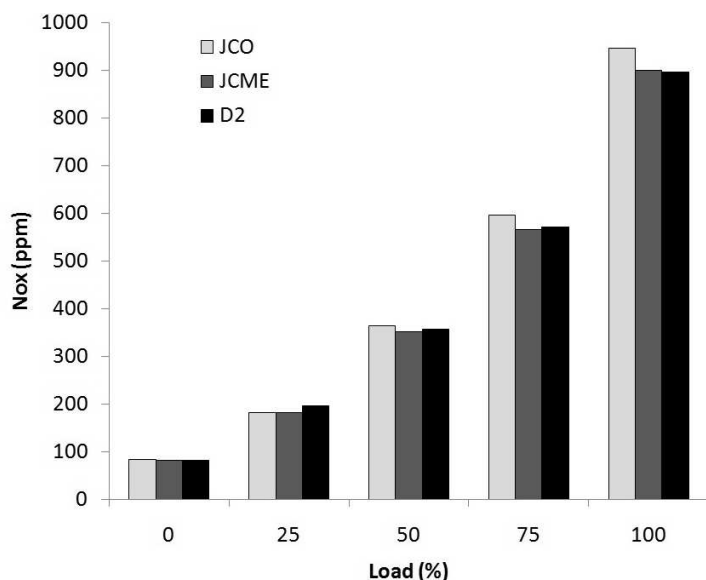


**Figure 5: NO<sub>x</sub> emissions for different fuel samples at different loads**

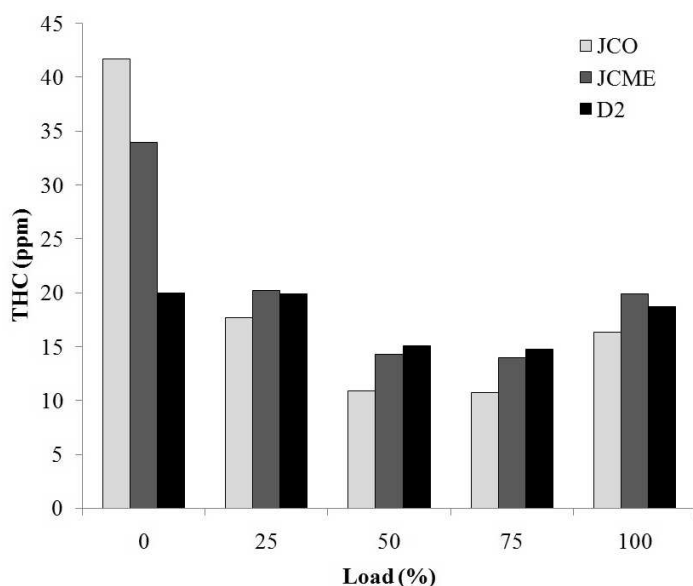


**Figure 6: THC emissions for different fuel samples at different loads**

since the fuel with oxygen may provide additional oxygen for the formation of NO<sub>x</sub> (Ramadhas *et al.*, 2005b).

### 3.6.2 Total hydrocarbons (THC)

The variation of THC emissions with loads is shown in Figure 6. It can be observed that THC emissions are maximum on idling, whereas lower THC values are obtained at 50% and 75% loads at steady engine speed. A similar trend was also observed in the literature, whereas high THC emission is observed at lower loads and maximum loads (Shi *et al.*, 2006). The small difference of D2 and JCME samples in THC emission could possibly be attributed to the higher fuel supply for a given load which produces slower combustion times and counteracts

the possible benefit of the presence of fuel borne oxygen in enhancing the combustion process of JCME (Aliyu *et al.*, 2011; Banapurmath *et al.*, 2008).

### 3.6.3 Carbon monoxide (CO)

The formation of CO with increasing load is illustrated in Figure 7. The figure shows that CO emission decreases with engine load. High CO emissions were observed at lower loads, with the lowest emissions recorded at 75% engine load. CO is a product of incomplete combustion; thus at higher engine loads, the higher combustion temperature promotes more complete combustion hence fewer CO emissions. The results of these CO emissions agree with those reported in the literature (Purushothaman and Nagarajan, 2009a; Banapurmath *et al.*, 2008). The relatively poor atomization and lower volatility of fuel samples is responsible for this trend. In addition, at lower loads, CO emissions are increased due to incomplete combustion, whereas at 100% load CO emissions are slightly increased compared to 75% load, due to the local presence of a richer mixture in the combustion chamber (Cheng *et al.*, 2008).

### 3.6.4 Carbon dioxide (CO<sub>2</sub>)

Fuel derived from vegetable oils reduces overall carbon dioxide in the atmosphere when it is used to run diesel engines, since plants absorb carbon dioxide during growth (Demirbas, 2008; Balat and Balat, 2008). Figure 8 illustrates CO<sub>2</sub> emission results. It can be observed that CO<sub>2</sub> emission increases as the load increases at the same engine speed. It can also be observed that JCO had the least CO<sub>2</sub> emissions followed by JCME then D2 in higher loads. Oxygen present in vegetable oils and biodiesel supports combustion hence, will lead to more CO<sub>2</sub> emissions at low loads due to complete combustion. This fact has been observed from literature (Mbarawa, 2008) as diesel exhibits lower CO<sub>2</sub> emissions. At higher loads, however, poor fuel atomization and lower combustion duration override the advantages of added oxygen in JCO and JCME and thus, incomplete combustion results.

### 3.6.5 Smoke

Smoke emissions results are shown in Figure 9. Diesel fuel recorded higher smoke emissions at all loads. Maximum smoke emission values were observed at 100% load for both fuels, where D2 fuel indicates the maximum value, while JCO recorded the minimum value under the same load condition. The presence of oxygen in JCO and JCME samples could explain their lower emission values (Chen *et al.*, 2008, Purushothaman and Nagarajan, 2009b).

## 3.7 Combustion analysis

The variation in injection timing exerts a major

influence on the engine performance and exhaust emissions. To understand and optimize the combustion process, a careful analysis of cylinder pressure and heat release has been performed, which furnishes precise information about the combustion process when using biodiesel. For this purpose, the experiments were carried out in a TDI compression ignition in order to analyse the combustion characteristics of the fuel samples tested.

### 3.7.1 Cylinder pressure

Figure 10 indicates the peak cylinder pressure for different fuels at different engine load conditions. Figure 11 illustrates the variations of cylinder pressure with crank angle degree (CAD) for the fuels at full load conditions and constant engine speed of 3000 rpm. Similar graphs were obtained at other loads with differences only in the magnitude of pressure and the corresponding crank angle in which it appears. In a CI engine, the cylinder pressure depends on the burned fuel fraction during the premixed burning phase, that is, the initial stage of combustion. Cylinder pressure characterizes the ability of the fuel to mix well with air and burn. High peak pressure and maximum rate of pressure rise correspond to the large amount of fuel burned in the premixed combustion stage (Agarwal, 2007).

It can be noted that JCO produced the least peak cylinder pressure, while JCME produced the highest at all loads. All fuels exhibited peak cylinder pressures between crank angles of  $-10^{\circ}$  and  $10^{\circ}$ , with lower load levels exhibiting peak cylinder pressure in negative crank angles and vice versa. It was also observed that the cylinder pressure increases as the load increases. This increase in pressure is to be expected in a TDI diesel engine. It is caused by the increased amount of injected fuel and charge pressure in the air intake manifold at higher loads. The temperature and volume flow of the exhaust gases that pass through the turbo charger influence the characteristics of air flow in the intake manifold, owing to the increased spinning speed of the turbocharger turbine and the heat exchange between exhaust gas and the charged air. The amount of air forced into the intake manifold increases as the load increases, since the high temperature, high velocity exhaust gas that passes through the turbocharger turbine causes a rise in the velocity of intake air, which forces more air into the cylinders. The increased amount of air causes larger amounts of fuel to be injected into the cylinder, which in turn, causes higher cylinder pressure.

JCME produced the highest peak pressures probably because of increase in ignition delay when using it. This ignition delay increases the amount of fuel burned within the premixed burning phase, causing high values of peak pressure and rate of pressure rise. JCME's lower viscosity (compared to JCO) and its contribution of intrinsic oxygen (com-

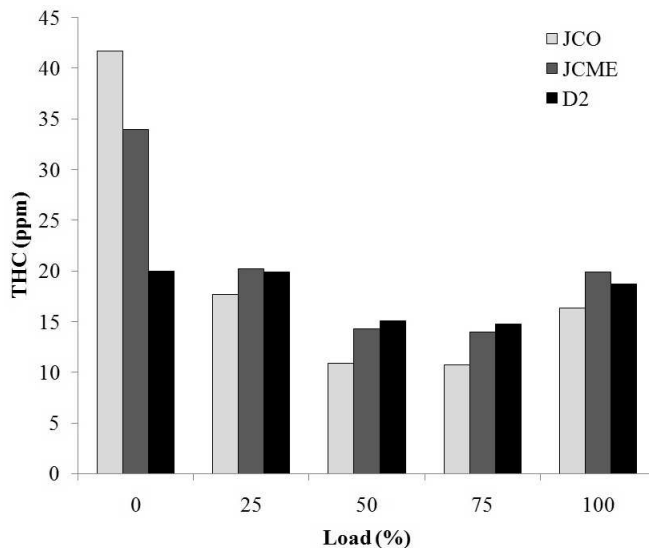


Figure 7: CO emissions for different fuel samples at different loads

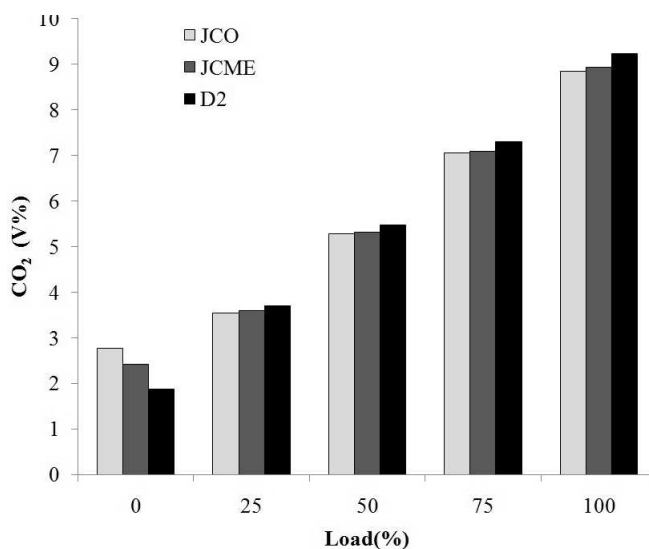


Figure 8: Carbon dioxide emission at different load conditions

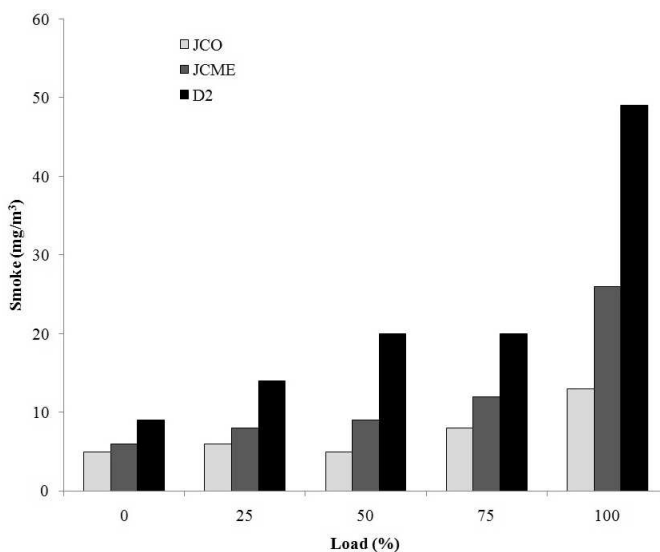
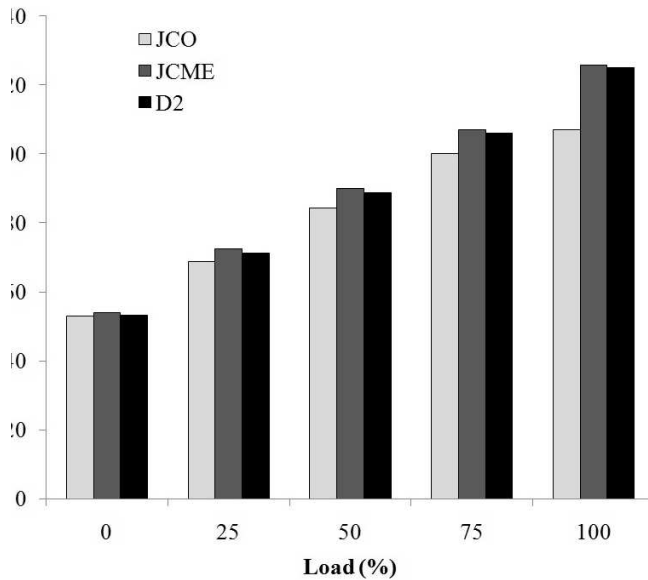
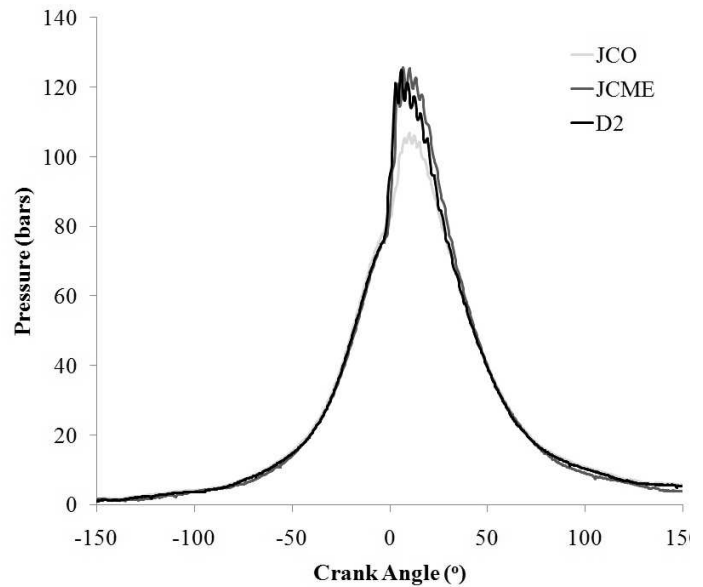


Figure 9: Smoke emissions for different fuel samples at different loads



**Figure 10: Peak cylinder pressure at different engine loads**



**Figure 11: Cylinder pressure variation with crank angle at full load**

pared to D2) may also be the reason for high cylinder pressure. High viscosity of JCO is the reason for its lower peak cylinder pressure, as the fuel spraying is affected by viscosity. Complete combustion depends to a large extent on fuel-air mixing. More complete combustion influences high cylinder pressure (Purushothaman and Nagarajan, 2009b; Purushothaman and Nagarajan, 2009a). Diesel (D2) indicates a slightly lower peak cylinder pressure than JCME, which may also be caused by oxygen-fuel mixing, which is more efficient in fuel that contains intrinsic oxygen (Agarwal, 2007; Ramadhas *et al.*, 2005b).

### 3.7.2 Heat release

Figure 12 depicts peak heat release rates for differ-

ent fuels. Figure 13 illustrates the variations of heat release with crank angle degree (CAD) for the fuels at full load conditions and constant engine speed of 3000 rpm. Similar graphs were obtained at other loads with differences only in the magnitude of heat release and the corresponding crank angle in which it appears.

All fuels follow a similar trend i.e. the peak heat release values increase as the load increases. This may be caused by high temperature and high cylinder pressure, better fuel-air mixing, and higher flame velocity associated with higher loads. All fuels experience rapid premixed burning followed by diffusion combustion, as is typical for naturally aspirated engines. After the ignition delay period, the premixed fuel air mixture burns rapidly, releasing

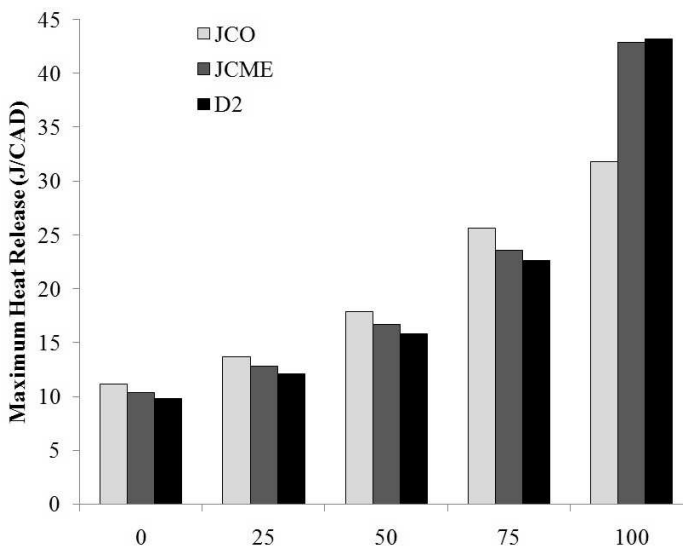


**Figure 12: Maximum rate of heat release at different engine loads**

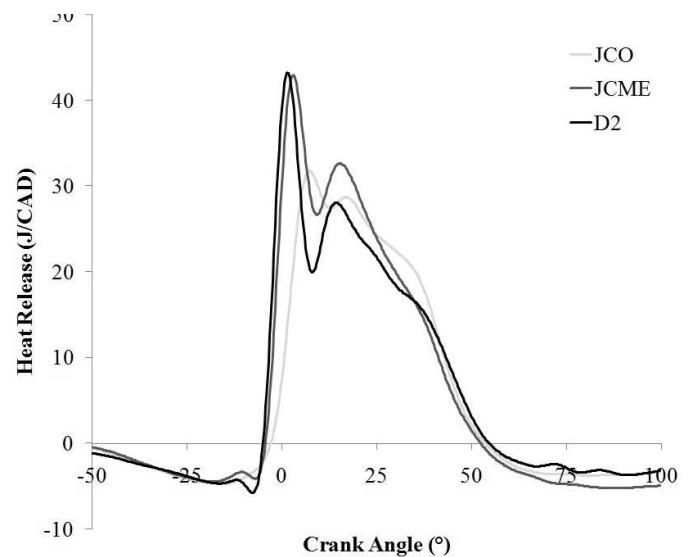


**Figure 13: Heat release variation with crank angle at full load**



heat at a very rapid rate, after which diffusion combustion takes place, where the burning rate is controlled by the availability of the combustible fuel-air mixture. It can be seen that JCO and JCME recorded an improvement in the heat release rate at the premixed combustion period. The presence of oxygen in these fuels decreased their cetane number and increased the ignition delay period. Therefore, while the engine was running with biodiesel, increased accumulation of fuel during the relatively longer delay period resulted in a higher rate of heat release. Even though D2 fuel exhibits high HV and lower viscosity, the intrinsic oxygen property of the other fuels influenced the heat release results observed. Because of the shorter delay period of diesel, its maximum heat release rate occurs earlier in comparison with JCME, while JCO was the last to exhibit its maximum heat release.

### 3.8 A summary of key findings

- The properties of methyl esters obtained using optimal parameters conformed to biodiesel standards (ASTM 6751 and EN 14214).
- The engine test results indicated that BSFC output from JCO and JCME were slightly weaker than those of mineral diesel; this is possibly due to their lower heating value compared to mineral diesel.
- The CO<sub>2</sub> and smoke emissions from mineral diesel were generally higher than JCME and JCO emissions. As for THC and CO emissions, it was affected by loading, where at lower loads, JCO had the highest emissions and at higher loads, D2 lead. NO<sub>x</sub> emissions were approximately the same for all fuels except in full load where JCO exhibited slightly higher emissions.
- Peak cylinder pressure and maximum heat release for all fuels increased with loadings where JCME exhibited the highest values in nearly all loads. The peak pressure and maximum heat were occurring at a range of crank angle between -10° and 10°. JCO had the least peak cylinder pressure whereas D2 had the least maximum heat release in nearly all loadings.

### 4. Conclusion

The foregoing analysis of fuel properties, engine performance, emissions characteristics, and combustion characteristics suggests that JCME can indeed be used as a fuel in diesel engines, resulting in reduced emissions and improved fuel properties and engine performance as compared to D2 fuel.

### References

Agarwal, A. K. (2007). Biofuels (alcohols and biodiesel) applications as fuels for internal combustion engines. *Progress in Energy and Combustion Science*, 33, 233-271.

Aliyu, B., Agnew, B. & Douglas, S. (2010). Croton megalocarpus (Musine) seeds as a potential source of bio-diesel. *Biomass and Bioenergy*, 34, 1495-1499.

Aliyu, B., Shitanda, D., Walker, S., Agnew, B., Masheiti, S. & Atan, R. (2011). Performance and exhaust emissions of a diesel engine fuelled with Croton megalocarpus (musine) methyl ester. *Applied Thermal Engineering*, 31, 36-41.

Balat, M. & Balat, H. (2008). A critical review of bio-diesel as a vehicular fuel. *Energy Conversion and Management*, 49, 2727-2741.

Banapurmath, N. R., Tewari, P. G. & Hosmath, R. S. (2008). Performance and emission characteristics of a DI compression ignition engine operated on Honge, Jatropha and sesame oil methyl esters. *Renewable Energy*, 33, 1982-1988.

Chen, H., Wang, J., Shuai, S. & Chen, W. (2008). Study of oxygenated biomass fuel blends on a diesel engine. *Fuel*, 87, 3462-3468.

Cheng, C. H., Cheung, C. S., Chan, T. L., Lee, S. C., Yao, C. D. & Tsang, K. S. (2008). Comparison of emissions of a direct injection diesel engine operating on biodiesel with emulsified and fumigated methanol. *Fuel*, 87, 1870-1879.

Demirbas, A. (2008). *Biodiesel: a realistic fuel alternative for diesel engines*, Springer Verlag.

Emil, A., Yaakob, Z., Satheesh Kumar, M., Jahim, J. & Salimon, J. (2010). Comparative Evaluation of Physicochemical Properties of Jatropha Seed Oil from Malaysia, Indonesia and Thailand. *Journal of the American Oil Chemists' Society*, 87, 689-695.

Foidl, N., Foidl, G., Sanchez, M., Mittelbach, M. & Hackel, S. (1996). Jatropha curcas L. as a source for the production of biofuel in Nicaragua. *Bioresource Technology*, 58, 77-82.

Heywood, J. B. (1998). *Internal combustion engine fundamentals*, New York, McGraw-Hill.

Keriko, J. M. (2007). *Bio-diesel Research and Production in Kenya*. Nairobi: Jomo Kenyatta University of Agriculture and Technology.

Knothe, G., van Gerpen, J. H. & Krahl, J. (2005). *The biodiesel handbook*. , Champaign, Illinois, AOCS Press.

Lalas, S. & Tsaknis, J. (2002). Characterization of Moringa oleifera Seed Oil Variety "Periyakulam 1". *Journal of Food Composition and Analysis*, 15, 65-77.

Lu, H., Liu, Y., Zhou, H., Yang, Y., Chen, M. & Liang, B. (2009). Production of biodiesel from Jatropha curcas L. oil. *Computers & Chemical Engineering*, 33, 1091-1096.

Makkar, H. P. S. & Becker, K. (2009). Jatropha curcas, a promising crop for the generation of biodiesel and value-added coproducts. *European Journal of Lipid Science and Technology*, 111, 15.

Mbarawa, M. (2008). Performance, emission and economic assessment of clove stem oil-diesel blended fuels as alternative fuels for diesel engines. *Renewable Energy*, 33, 871-882.

Mogaka, V. M., Iiyama, M., Mbatia, O. L. E. & Jonathan, N. (2010). Reality or romanticism? Potential of Jatropha to solve energy crisis and

- improve livelihoods. In: Joint 3rd African Association of Agricultural Economists (AAAE) and 48th Agricultural Economists Association of South Africa (AEASA) Conference, September 19-23 2010 Cape Town, South Africa. 1-30.
- Pramanik, K. (2003). Properties and use of jatropha curcas oil and diesel fuel blends in compression ignition engine. *Renewable Energy*, 28, 239-248.
- Purushothaman, K. & Nagarajan, G. (2009a). Experimental investigation on a C.I. engine using orange oil and orange oil with DEE. *Fuel*, 88, 1732-1740.
- Purushothaman, K. & Nagarajan, G. (2009b). Performance, emission and combustion characteristics of a compression ignition engine operating on neat orange oil. *Renewable Energy*, 34, 242-245.
- Ramadhas, A. S., Jayaraj, S. & Muraleedharan, C. (2005a). Biodiesel production from high FFA rubber seed oil. *Fuel*, 84, 335-340.
- Ramadhas, A. S., Muraleedharan, C. & Jayaraj, S. (2005b.) Performance and emission evaluation of a diesel engine fueled with methyl esters of rubber seed oil. *Renewable Energy*, 30, 1789-1800.
- Rashid, U., Anwar, F., Moser, B. R. & Knothe, G. (2008). Moringa oleifera oil: A possible source of biodiesel. *Bioresource Technology*, 99, 8175-8179.
- Ren, Y., Huang, Z., Miao, H., Di, Y., Jiang, D., Zeng, K., Liu, B. & Wang, X. (2008). Combustion and emissions of a DI diesel engine fuelled with diesel-oxygenate blends. *Fuel*, 87, 2691-2697.
- Shi, X., Pang, X., Mu, Y., He, H., Shuai, S., Wang, J., Chen, H. & Li, R. (2006). Emission reduction potential of using ethanol-biodiesel-diesel fuel blend on a heavy-duty diesel engine. *Atmospheric Environment*, 40, 2567-2574.
- Tomomatsu, Y. & Swallow, B. (2007). Jatropha curcas biodiesel production in Kenya. Nairobi: World Agroforestry Centre.
- Treese, J. V., Paper, M., Li, Y., Wang, Q. & Moore, K. (2010). Jatropha curcas Cultivation and Use as a Biodiesel Feedstock. Florida: University of Florida.
- Tsaknis, J., Lalas, S., Gergis, V., DourtogloU, V. & Spiliotis, V. (1999). Characterization of Moringa oleifera variety Mbololo seed oil of Kenya. *Journal of Agricultural Food Chemistry* 47, 4495-4499.
- Wagutu, A., Chhabra, S., Thoruwa, C., Thoruwa, T. & Mahunnah, R. (2009). Indigenous Oil Crops As A Source For Production Of Biodiesel In Kenya. *Bulletin of the Chemical Society of Ethiopia*, 23, 359-370.

Received 3 May 2012; revised 10 March 2014